Conservation of Bond Order during Radical Substitution Reactions: Implications for the BEBO Model

Paul Blowers and Richard I. Masel*

Department of Chemical Engineering, University of Illinois at Urbana-Champaign, Urbana, Illinois 61801-3792

Received: July 8, 1998; In Final Form: September 2, 1998

The bond energy−bond order model has been used extensively to predict behaviors and energetics of species where ab initio calculations are still too expensive. However, the accuracy of bond order conservation, even for small polyatomic systems, is still unknown. In this paper, we use ab initio calculations at the PMP2 = (full)/6-31 g* and G-2 level to examine bond order conservation for the following gas-phase radical substitution reactions: $H^* + CH_3OH \rightarrow CH_3H^* + OH$, $H^* + CH_3OH \rightarrow HOH^* + CH_3$, $H^* + CH_3OH \rightarrow HH^* + CH_2OH$, $H^* + CH_3OH \rightarrow HH^* + CH_3O$, $H^* + CH_3OH \rightarrow H + CH_2H^*OH$, $H^* + CH_3OH \rightarrow H + CH_3OH^*$. We find that total bond order is approximately conserved during atom transfer reactions, but is not conserved during the more complicated hydrogenolysis reactions or during hydrogen exchange on oxygen. An early transition state is predicted for hydrogen exchange on oxygen, and late ones for the hydrogenolysis reactions. Even though the transition state structures may differ greatly from the ab initio predictions, the barrier heights predicted with bond order conservation are only incorrect by 1−2 kcal/mol. This behavior arises because the potential energy surfaces are relatively flat in the region where the transition states are found. Consequently, the energies of the transition state predicted with either method are in close agreement, even though the structures are poorly represented by bond order conservation methods.

Introduction

The bond energy−bond order (BEBO) method introduced by Johnston and Parr[1−3] has been used extensively to predict chemical phenomena since it was first introduced in 1967. The BEBO model is essentially an empirical method that yields energies of species as a function of bond strengths and bond lengths via the bond order as defined by Pauling.[4]

Initially, the BEBO model was used to describe the reactive behavior of small sized systems and to predict the energies of species.[5−9] This type of use also led to the development of qualitatively correct potential energy surfaces for simple reactions.[10,11] As ab initio calculations were developed, it became possible to model these simple systems more exactly with quantum mechanics. However, larger systems are still too calculationally expensive for ab initio calculations to handle, and the BEBO model is used instead.[12−15]

One key assumption of the BEBO model is that the total bond order of the system remains constant throughout a reaction. This same assumption is also a key underpinning of the UBI-QEP and BOC-MP methods proposed by Shustorovich and Sellers[16−20] to describe surface phenomena. These surface problems are still mostly too expensive to examine fully with quantum mechanics, and assumptions, like bond order conservation, are often made to evaluate energetic behavior.

As ab initio calculations have become cheaper through code and computer architecture improvements, the validity of bond order conservation has been investigated. So far, gas-phase three-center linear reactions,[21−23] gas-phase isomerizations,[24−27] small group transfer reactions in the gas phase,[28−30] and pericyclic reactions[31] have been studied. Also, its validity has been verified for diatomic dissociation on some metal surfaces.[20] Most of the reactions examined so far involve highly symmetric behavior during the reaction, where the forming and breaking bonds are essentially equivalent, which may lead to better bond order conservation.

The forming and breaking bond order curves have been used to predict the location of the transition state. The transition state has previously been located at the inflection point of the forming and breaking bond order curves[25−27] for three-center isomerization reactions. On the other hand, the transition state has also been found to lie at the minimum of the total bond order curve for polyatomic atom reactions.[28] If it is possible to use bond order curves to predict the structures of transition states, computational effort could be reduced.

In this paper, the gas-phase reaction of radical hydrogen with methanol was used to examine the validity of bond order conservation during symmetric and asymmetric reactions. The six reactions studied were:

$$H^* + CH_3OH \rightarrow CH_3H^* + OH \quad (1)$$

$$H^* + CH_3OH \rightarrow HOH^* + CH_3 \quad (2)$$

$$H^* + CH_3OH \rightarrow HH^* + CH_2OH \quad (3)$$

$$H^* + CH_3OH \rightarrow HH^* + CH_3O \quad (4)$$

$$H^* + CH_3OH \rightarrow H + CH_2H^*OH \quad (5)$$

* Author to whom correspondence should be addressed.

10.1021/jp9829243 CCC: $15.00
Published on Web 10/29/1998

$$H^* + CH_3OH \rightarrow H + CH_3OH^* \quad (6)$$

All six of these reactions are bimolecular radical substitutions. In reactions 1 and 2 the C−O bond is involved, while the C−H bond is involved for reactions 3 and 5. Reactions 4 and 6 involve the O−H bond. The structures of the transition states were found at the MP2 = (full)/6-31 g* level and are compared to those predicted from bond order arguments. The intrinsic reaction pathways are also compared to the bond order conserved pathways, which yield information about the degree of passivity of spectator bonds. Finally, barrier heights and the location of the transition states from both ab initio and bond order conserved methods are compared to evaluate the ability of bond order conservation to correctly predict structures and barrier heights to reaction.

Computational Methods

The Gaussian 92 and Gaussian 94 packages were used for all calculations in this work.[32,33] All geometry optimizations were performed using the MP2 = (full)/6-31 g* basis set, and spin contamination was eliminated with spin projection. Frequency calculations verified that all transition states were first-order saddle points with only one negative eigenvalue in the Hessian matrix. Intrinsic reaction coordinate calculations were done starting at the transition state geometries in order to follow the reaction pathways toward reactants and products. Potential energy surfaces, which are also described elsewhere,[34,35] were generated for each reaction to reveal any unusual features. Here, the forming and breaking bond lengths were fixed, and all other geometry parameters were optimized as described elsewhere.[34,35] All stationary point and IRC energy calculations were done at the G-2 level. In previous work[34−38] we tried various basis sets and computational methods and found that G-2 gives the most reliable energies for this system.

The bond order as defined by Pauling[4]

$$n = \exp\left(\frac{-(R - R_{eq})}{a}\right) \quad (7)$$

was used; where n is the bond order at some bond length, R, compared to an equilibrium bond length, R_{eq}. The constant, a, has been reported to have values ranging from 0.2 to 0.4, with 0.26 most frequently used.[21−30] While others have argued that a should vary with R_{eq}, a value of 0.3 was chosen for this work. Values of a larger than 0.3 moved the transition states later, while smaller values moved the transition state earlier.

Bond order conservation was stipulated by requiring that the sum of the forming, n_f, and breaking, n_b, bond orders equals one:

$$n_t = n_b + n_f = 1 \quad (8)$$

Bond order conserved pathways were found by using R_f from the intrinsic reaction coordinate calculations to find n_f. Then, R_b was found by using eq 7 while satisfying eq 8. Energies along the bond order conserved pathways were found by fixing the forming and breaking bond lengths at these bond order conserved values before optimizing the other geometry parameters.

The bond order for the passive bonds, i.e., those not explicitly forming or breaking during the reaction, required the use of a monotonically changing function for the equilibrium bond length. For example, consider the carbon−oxygen bond for reaction three as shown in Figure 1. At the beginning of the reaction, the equilibrium bond length of C−O is 1.423 Å for methanol. This bond length shrinks to 1.3731 Å at the product, CH_2OH. To avoid discontinuities in the passive bond order curves at the transition state by switching R_{eq} values suddenly, R_{eq} was assumed to vary linearly from reactants to products. Note, however, that this method was not needed for reactions 5 and 6 where methanol is both the product and reactant.

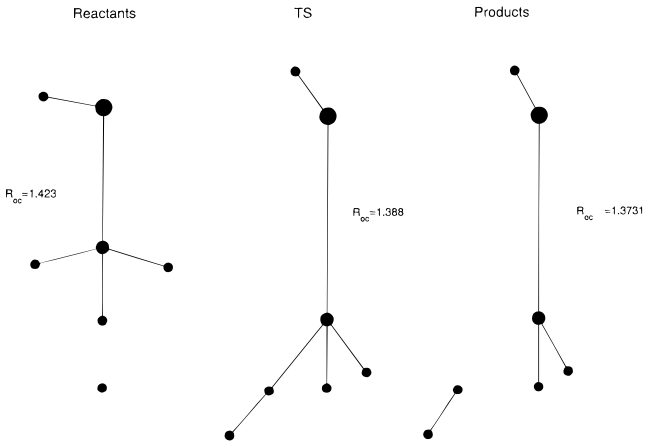

Figure 1. The variation of $R_{oc,eq}$ along the reaction coordinate for H* + CH_3OH → HH* + CH_2OH. Lengths are in angstroms.

The locations of the inflection points in the bond order curves for the forming and breaking bonds were found using the intrinsic reaction coordinate calculation geometry information. A third-order polynomial was fit to each bond order curve in the range where the curvature was expected to change. This was between −0.8 and 0.8 on the reaction coordinate scale. The root of the second derivative of the bond order curve polynomial is where the inflection point lies.

Results

The potential energy surfaces generated for this work are shown in Figure 1. The transition state is indicated by "TS" and all contours are scaled 5 kcal/mol apart. For some reactions, like reactions 1, 2, and 6, it was necessary to impose some additional geometry constraints to stay on the correct reaction sheet. Here, we use the term reaction sheet to denote a potential energy surface that connects the correct products to the desired reactants. In these cases, additional bonds were held constant to prevent the molecule from fragmenting. The areas where this was necessary are denoted with a dashed box.

These potential energy surfaces look like what one expects for S_N2 reaction with no unusual features. The transition state lies at the lowest barrier height that links products to reactants. In this study, most product and reactant pathways connecting the transition states with the infinitely separated species contain stable complexes. This is not unusual for reactions of this type and does not lead to any unusual features on these energy surfaces. This indicates these six reactions are good test cases for bond order conservation validity for S_N2 reactions.

Figure 2 shows the forming bond order, breaking bond order, and total bond order versus the reaction coordinate. Notice that the hydrogenolysis reactions, eqs 1 and 2, show large variations from bond order conservation where the total bond order should equal one. Also, hydrogen exchange on oxygen shows large deviations from 1, but is always positive in this case. Table 1 summarizes the average absolute total bond order error where

$$\text{A.E.} = \sum \left| \frac{n_t - 1.0}{\#\text{points}} \right| \quad (9)$$

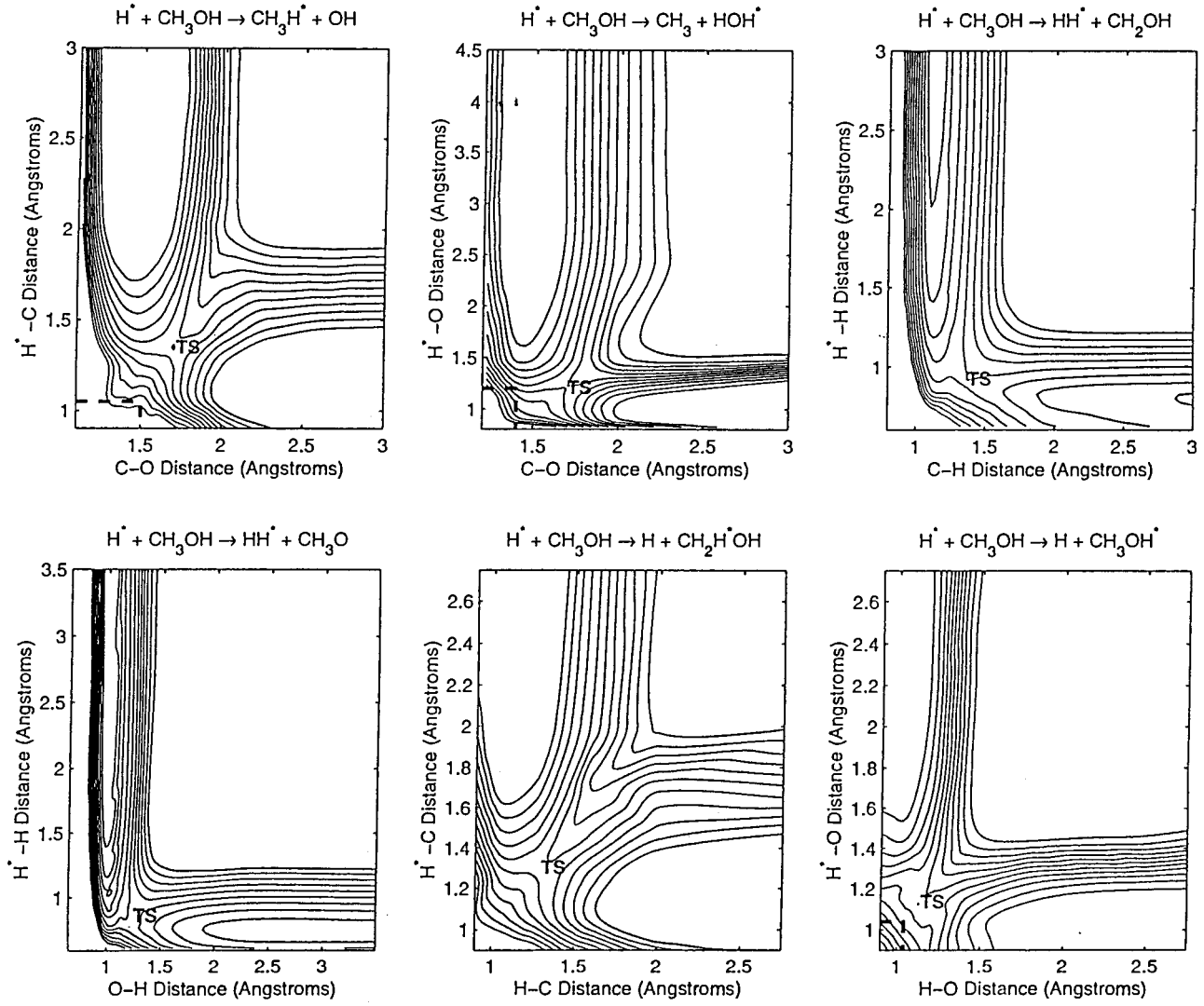

Figure 2. The potential energy surfaces for H + CH_3OH → products. "TS" indicates the location of the transition state. All contours are 5 kcal apart. Dashed boxes indicate where geometry constraints were imposed to stay on the same reaction sheet.

TABLE 1: Average Absolute Errors of Total Bond Conservation for H* + CH_3OH → Products, Using the Forming and Breaking Bond Orders

reaction	average absolute error
1	0.197
2	0.192
3	0.056
4	0.090
5	0.036
6	0.114

We see that the hydrogenolysis reactions show the largest deviations from bond order conservation, while hydrogen exchange on carbon and the hydrogen abstraction reactions are relatively conserved.

Figure 3 shows a plot of the passive bond orders as a function of reaction coordinate. Once again, equilibrium bond lengths were scaled along the reaction pathway to avoid discontinuities as the bond lengths changed throughout the reaction. The C−O bond order is shown with a dark dashed line, the out-of-plane H−C bonds are shown with asterisks, the O−H bond by a solid line, and the in-plane C−H bond is shown with open circles.

We see that all passive bonds are essentially conserved. Only the C−O bond order during hydrogen exchange on oxygen shows large deviations from 1.0. Table 2 shows the average absolute errors for passive bonds.

Table 3 shows the locations of the inflection points of the forming and breaking bond order curves. The transition state should be where the reaction coordinate is zero based on the intrinsic reaction coordinate calculations. We see that there is no inflection point for the forming bond in reaction 1. The prediction of one for reaction 2 is an artifact of a little dip in the curve within the range of data chosen for polynomial fitting. Using a wider range of data for this case led to an inflection point outside the range of the plot. The breaking bond order curve for these two hydrogenolysis reactions would predict the transition state to lie earlier than it actually does. In the third and fourth reactions, the inflection point is much later than the transition state for the forming bond while it is just slightly early for the breaking bond. This trend is reversed for hydrogen exchange on carbon. The last reaction shows the best agreement between the location of the transition state and the location of the inflection point with differences of only 0.005 along the reaction coordinate.

Varying the range of data used to fit to the polynomials and changing the highest order of the polynomial used in the fit did not improve the ability of bond order curves to predict where the transition state should be. Higher-order polynomials only generated more roots to the polynomial fit, and most of these

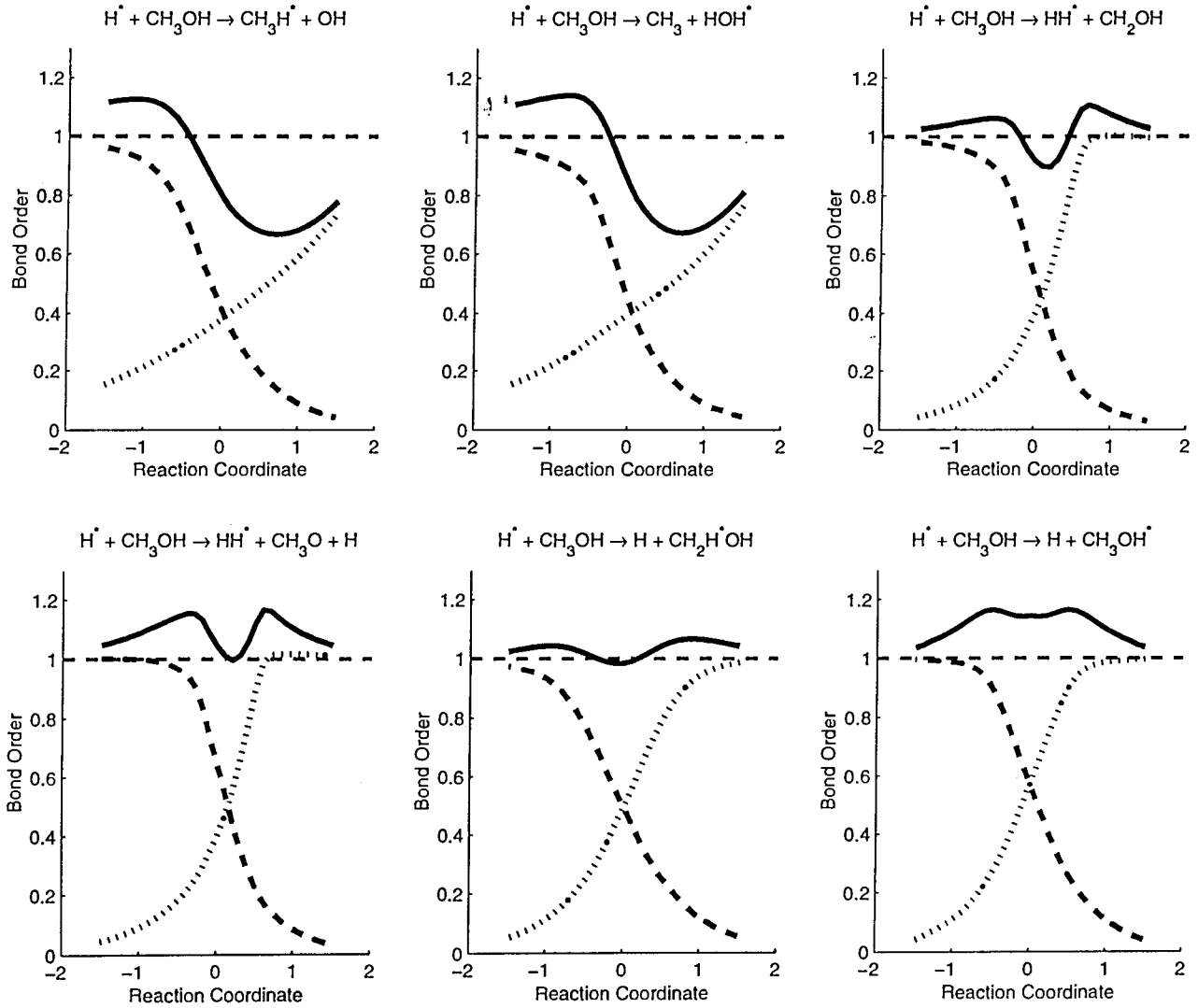

Figure 3. Total bond order (solid line), forming bond order (dotted line), and breaking bond order (dashed line) for H + CH_3OH → products versus reaction coordinate. Geometries are from MP2 = (full)/6-32 g* intrinsic reaction coordinate calculations.

TABLE 2: Average Absolute Error in Passive Bond Order Conservation for H* + CH_3OH → Products

	average absolute error for passive bonds				
reaction	O−H	C−H (in plane)	C−H (out-of-plane)	C−H (out-of-plane)	C−O
1	0.0051	0.0076	0.0183	0.0297	not passive
2	0.0225	0.0066	0.0072	0.0162	not passive
3	0.0018	not passive	0.0102	0.0119	0.0254
4	not passive	0.0129	0.0044	0.0162	0.0082
5	0.0089	not passive	0.0056	0.0217	0.0599
6	not passive	0.0106	0.0253	0.0253	0.1209

new roots were more than one unit away from the transition state on the reaction coordinate scale. This artifact was caused by the waves generated in the bond order fit.

In Figure 4, the potential energy surfaces are replotted on a smaller scale and the reaction pathways have been added. The solid line is the intrinsic reaction pathway, and its transition state is marked by "TS". The dashed line represents the bond order conserved pathway, with "X" denoting the transition state. We see that the two pathways are in good agreement for the hydrogen abstraction reactions and for hydrogen exchange on carbon. The largest deviations between the two pathways are for reactions 1 and 2. The locations of the transition states as predicted by both models are also farthest away for these two reactions. Hydrogen replacement on oxygen, too, shows slight deviations from the intrinsic pathway.

TABLE 3: The Location of Inflection Points in the Forming and Breaking Bond Order Curves and Predicted through Third-Order Polynomial Fits of Bond Order Data in the −0.8 < Reaction Coordinate < 0.8 Range

	location of inflection point on reaction coordinate scale	
reaction	forming bond	breaking bond
1	not available	−0.216
2	−0.043	−0.089
3	0.398	−0.021
4	0.364	0.089
5	−0.104	0.091
6	−0.006	0.005

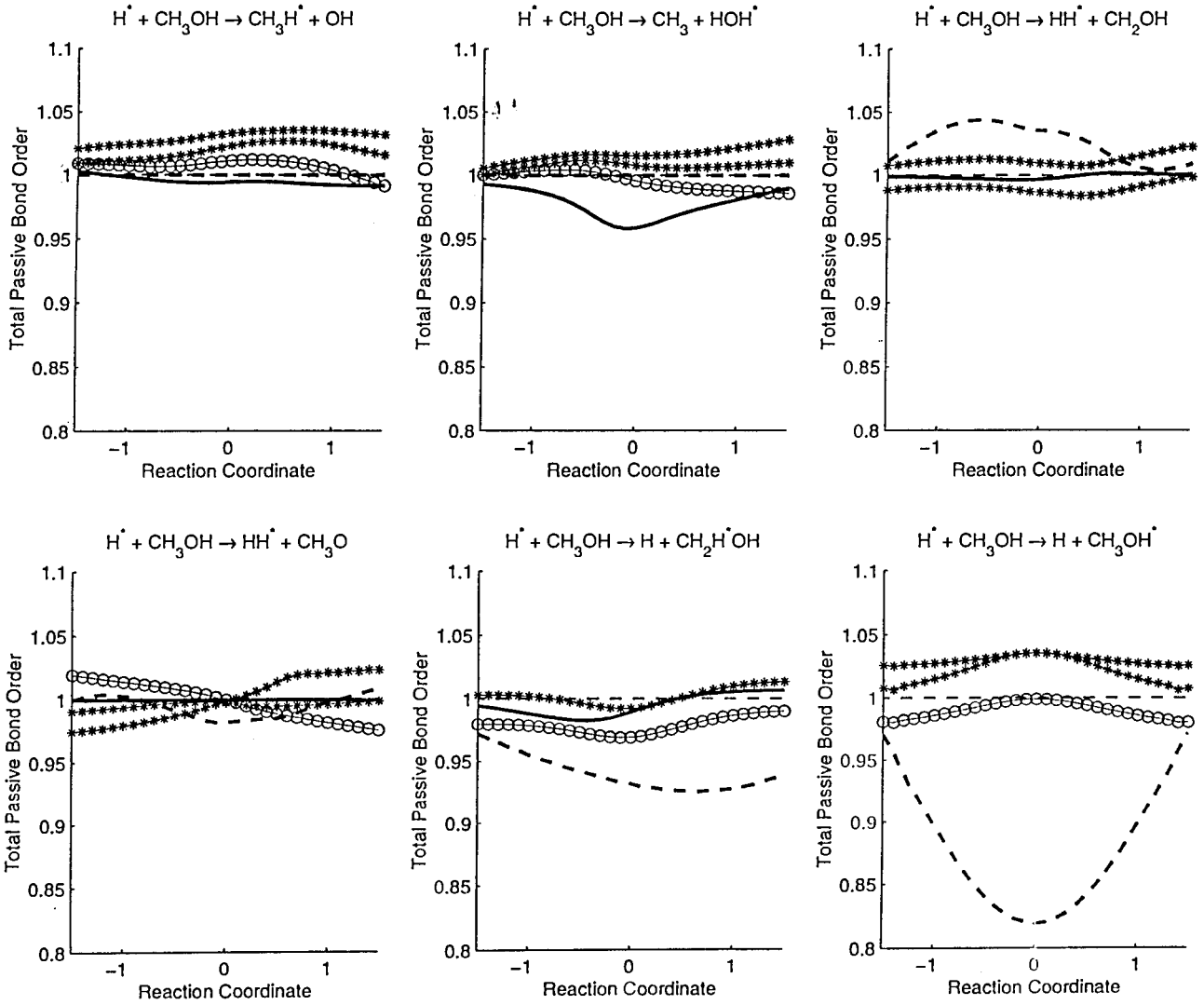

Figure 4. Passive bond orders plotted versus the reaction coordinate. Asterisks indicate out-of-plane C−H's, dashed line is for C−O, solid is for O−H, and the in-plane C−H is represented by open circles.

TABLE 4: Energies of the Barrier Height with Respect to the Reactant Energy (kcal/mol)[a]

reaction	G-2 barrier height	BEBO barrier height
1	48.99	49.90
2	39.45	40.49
3	20.17	19.83
4	26.56	26.69
5	54.84	54.92
6	43.05	43.63

[a] Calculated at the G-2 level and with the BEBO approximation.

Figure 5 is a plot of the energy of the species versus bond order. The intrinsic reaction pathway energies are represented by the solid black line, while the dashed line shows the bond order conserved pathway. The bond order conserved pathway was obtained by satisfying eq 8 with appropriate bond lengths before optimizing the other geometry constraints.

The maximum energy along each pathway represents the location and height of the barrier to reaction. We see that the locations and heights of the transition state are virtually identical for the hydrogen abstraction reactions and for hydrogen exchange on carbon. Barrier heights with both methods are shown in Table 4. The transition state is predicted to be too late using the bond order conserved pathways for the hydrogenolysis reactions. Hydrogen exchange on oxygen, on the other hand, has an earlier transition state with the bond order conserved pathway. Despite the errors in transition state location, the barrier heights are within 2 kcal for each method.

Discussion

We have found that bond order is not conserved during some reactions. Table 1 and Figure 3 both show that reactions 1 and 2 have total bond orders that are not conserved during the reaction. Previous researchers[21−30] have claimed that bond order can be considered to be conserved when the total bond order remains between 0.9 and 1.1. For the two hydrogenolysis reactions, total bond order is as low as 0.7. Also, hydrogen exchange on oxygen, reaction 6, deviates too far from 1.0, with values approaching 1.2.

For reactions 1 and 2, the breaking bond initially does not change much, even as the forming bond steadily shortens. This leads to a rise in total bond order. Then, the breaking bond extends very rapidly, leading to a corresponding drop in total bond order until the bond is essentially broken. The breaking bond order finally levels off as the forming bond continues to rise and the total bond order increases again.

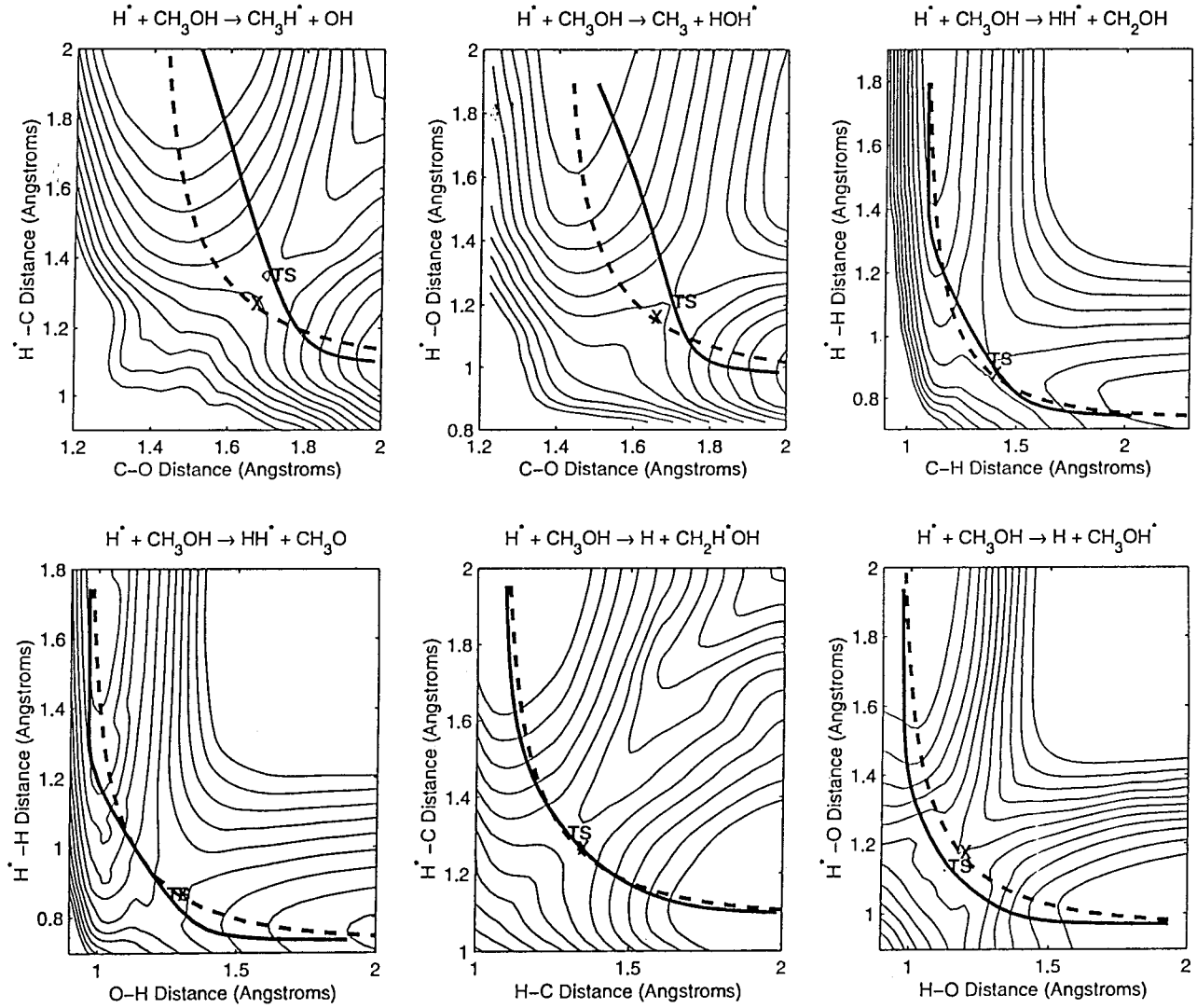

Figure 5. The reaction pathways from bond order conserved (dashed line) with the transition state (X) and the intrinsic reaction (solid line) calculation with the transition state (TS). All contours are 5 kcal apart.

For reaction 6, at long distances, the tails of the forming and breaking bond order curves are not as level as they are at short distances. This leads to total bond orders greater that 1.0 at the beginning and end of the reaction.

Now, let us consider how the spectator bond orders change during reaction. Figure 4 showed the bond orders of the passive bond orders during the reaction. Keep in mind that the equilibrium bond lengths used in eq 7 were varied along the reaction coordinate to account for changes in the species. However, this was not needed for reactions 5 and 6 because methanol was both the reactant and product of interest. We see that most passive bond orders remain very close to one. The carbon−oxygen bond, though, shows very large deviations from 1.0 for reaction 6.

The bond order for the C−O bond during hydrogen exchange on oxygen drops to a value of 0.825 at the transition state. Since spectator bonds are not involved in the reaction, one would expect this value to remain much closer to 1.0. Physically, the C−O bond elongates as the hydrogen approaches. This is driven by electron−electron repulsions as the species attempts to minimize energy. The transition state is starting to look like a methyl−water species, i.e., $CH_3 + OH_2$ more than it looks like a methanol species. The BEBO model requires that spectator bonds that are not involved in the reaction remain constant. However, we see here that this is definitely not true for the carbon−oxygen bond during hydrogen exchange on oxygen.

Maity et al.[25−27] claimed that the transition state would be located at the inflection point of the forming and breaking bond order curves. Table 3 showed our results considering data from −0.8 to 0.8 on the reaction coordinate, with the transition state lying at 0.0. We see that the forming bond for reactions 1 and 2 does not have an inflection point. The one that is found is an artifact of a dip in the data and does not represent the overall trend in the data. The breaking bond order inflection points for these two reactions would predict much earlier transition states than the intrinsic reaction coordinate calculations show.

The location of the forming bond order inflection point gives much later transition states for the hydrogen abstraction reactions, placing the transition state at about 0.4 on the reaction coordinate axis. The breaking bond would predict a slightly early transition state for reaction 3 and a considerably late one for reaction 4. In fact, the only reaction which appears to have inflection points near the transition state is reaction 6.

While some researchers have used the inflection point in forming and breaking bond orders to describe transition state structures, this analysis shows that the true transition state may be found far from the inflection points. Because these deviations are so large, the location of the inflection points in the bond

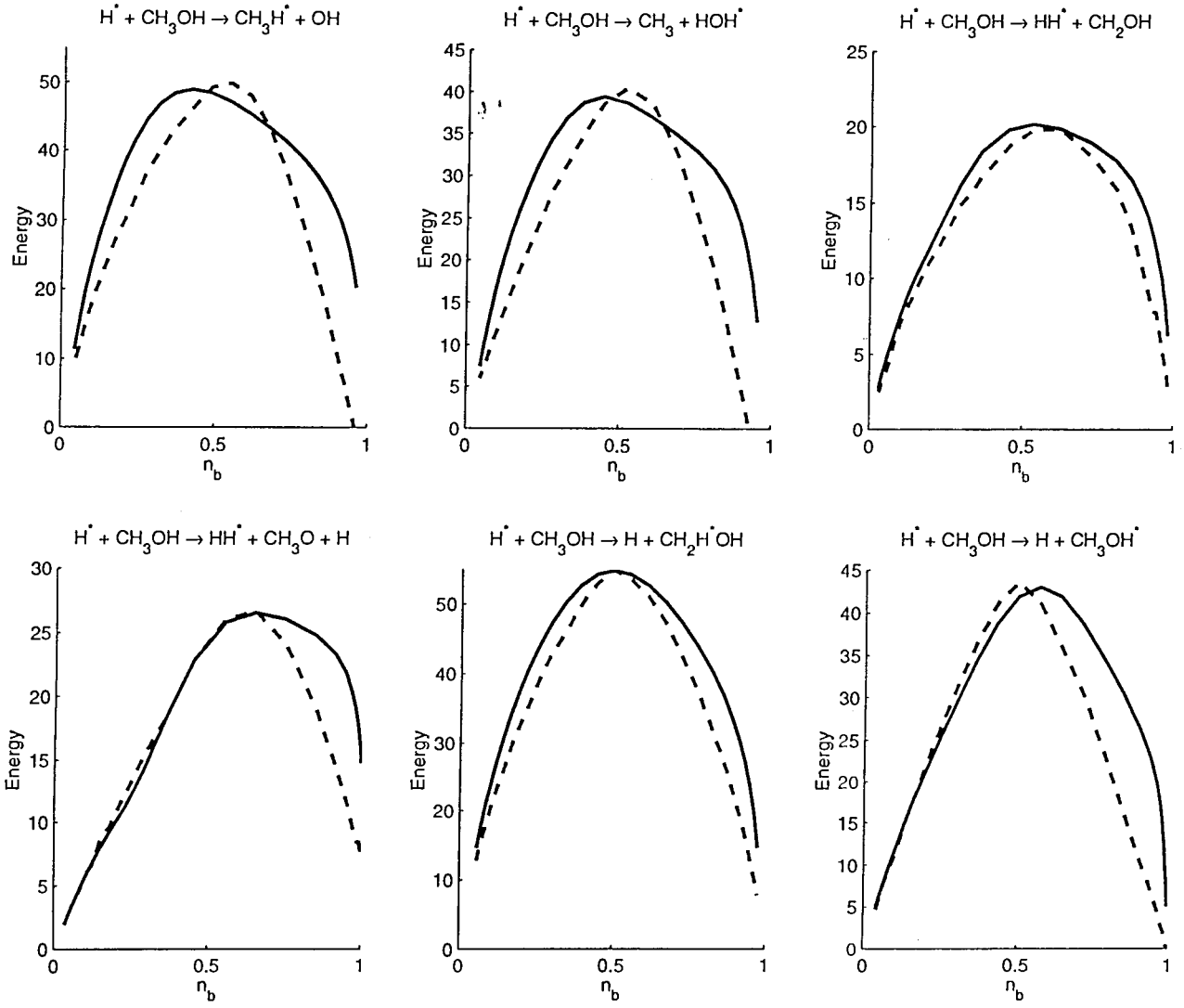

Figure 6. G2 energies along the bond order conserved (dashed line) and intrinsic reaction coordinate (solid line) pathways versus bond order. Energies are with respect to reactant energies (kcal/mol).

order curves are not recommended as a way of determining saddle point structures.

Figure 5 showed the reaction paths predicted from ab initio methods and bond order conserved arguments. The largest deviations between the two pathways are for reactions 1 and 2. The pathways are widely different in the beginning of the reaction, but are much closer toward the products. The locations of the transition states are also very different. The other reactions show much closer agreement between the two methods, with only reaction 6 differing slightly. In reaction 6, the bond order conserved pathway has a tighter curvature which could change the rate predicted if this pathway were used instead of the ab initio one.

Finally, Figure 6 shows that the barriers predicted with either method are very close to one another. While the bond order conserved pathway predicts transition states which are slightly late for reactions 1 and 2 and early for reaction 6, the barrier heights are essentially correct, being only 2 kcal away from the ab initio values.

Figure 4 shows why the barrier heights are close to the ab initio values even though the structures are considerably different. Notice that the potential energy surfaces are relatively flat near the transition states. The energy differences between the two methods, then, are not that great even though the transition states may lie as much as a tenth of an angstrom apart.

The results found for the six reactions studies have a few implications for the BEBO model. We find that the passive bonds are indeed passive for most of the reactions. However, the carbon−oxygen bond changes substantially during hydrogen exchange on oxygen. This may lead to problems if the BEBO model was used. A more correct formulation of the BEBO model should take into account these large deviations and the changes in energy that result.

We also find that geometries are not well represented by the bond order conserved pathway along the reaction coordinate, particularly at the transition state. This was especially evident for the hydrogenolysis reactions. This implies that bond order conserved geometries should be verified with ab initio calculations if anything other than the barrier height is desired. For instance, the ab initio structure would be needed for frequencies used to predict reaction rates.

Despite the geometries being incorrect, the barrier heights predicted with each method were within 2 kcal of each other. This agreement between the two methods shows that bond order conservation is a reasonable approximation if one wants to

estimate the barrier height at the transition state for reactions with flat barriers.

Conclusions

In summary, in this paper we used ab initio calculations to assess the validity of bond order conservation for several types of reactions. The reactions studied include hydrogenolysis reactions, hydrogen exchange reactions, and simple hydrogen transfer reactions. We find that the bonds not involved with the reaction were mostly passive, except for the hydrogen exchange reaction on oxygen where the carbon−oxygen bond elongated to accommodate the transition state structure.

We also find that the inflection points on the bond-forming and -breaking bond order curves are not good representations of the transition state locations. In some cases, there is no inflection point. In other cases, the forming and breaking bond order curve inflection points incorrectly predict the location of the transition state. In only one case did we find good agreement with ab initio calculations.

We also show that the bond order conserved pathways give incorrect geometry descriptions of the transition state for half of the reactions. The hydrogenolysis reactions show the largest errors, while symmetric hydrogen exchange on carbon shows very little error. Despite the incorrect geometry predictions, the barrier heights predicted with the bond order conserved pathway and ab initio calculations are within 2 kcal of each other because the barriers are so flat.

Acknowledgment. This work was funded by NSF Grant CTS 96 10115.

References and Notes

(1) Johnston, H. S. *Adv. Chem. Phys.* **1960**, *3*, 131.
(2) Johnston, H. S.; Parr, C. *J. Am. Chem. Soc.* **1960**, *85*, 2544.
(3) Johnston, H. S. *Gas-Phase Reaction Rate Theory*; Ronald Press: New York, 1966.
(4) Pauling, L. *J. Am. Chem. Soc.* **1947**, *69*, 542.
(5) Johnston, H. S.; Heicklen, J. *J. Phys. Chem.* **1962**, *66*, 532.
(6) Sullivan, J. H. *J. Chem. Phys.* **1963**, *39*, 3001.
(7) Schneider, F. W.; Rabinovich, B. S. *J. Am. Chem. Soc.* **1962**, *84*, 4215.
(8) Caldon, E. F.; Harbran, E. *J. Chem. Soc.* **1962**, 3454.
(9) Gilliom, R. D. *J. Chem. Phys.* **1976**, *65*, 5027.
(10) Agmon, N. *Chem. Phys. Lett.* **1977**, *45*, 343.
(11) Agmon, N. *J. Chem. Faraday Trans. 2* **1977**, *74*, 388.
(12) Berti, P. J.; Blanke, S. R.; Schramm, V. L. *J. Am. Chem. Soc.* **1997**, *119*, 12079.
(13) Rising, K. A.; Schramm, V. L. *J. Am. Chem. Soc.* **1997**, *119*, 27.
(14) Kline, P. C.; Schramm, V. L. *Biochemistry* **1993**, *32*, 13212.
(15) Aristov, N.; Armentrout, P. B. *J. Am. Chem. Soc.* **1984**, *106*, 4065.
(16) Shustorovich, E.; Sellers, H. *Surf. Sci. Rep.* **1998**, *31*, 1.
(17) Shustorovich, E. *Surf. Sci. Rep.* **1986**, *6*, 1.
(18) Sellers, H. *J. Phys. Chem.* **1994**, *98*, 968.
(19) Sellers, H. *Surf. Sci.* **1994**, *310*, 281.
(20) Sellers, H.; Shustorovich, E. *Surf. Sci.* **1996**, *346*, 322.
(21) Murdoch, J. R. *J. Am. Chem. Soc.* **1983**, *105*, 2667.
(22) Wolfe, D. J.; Mitchell, J.; Schlegel, H. B. *J. Am. Chem. Soc.* **1981**, *103*, 7986.
(23) Dunning, T. H., Jr.; Harding, L. B.; Bair, R. A.; Eades, R. A.; Shephard, R. A. *J. Phys. Chem.* **1986**, *90*, 344.
(24) Lendvay, G. *J. Phys. Chem.* **1989**, *93*, 4422.
(25) Maity, D. K.; Majumdar, D.; Bhattacharyya, S. P. *J. Mol. Struct. (THEOCHEM)* **1992**, *276*, 315.
(26) Maity, D. K.; Bhattacharyya, S. P. *J. Am. Chem. Soc.* **1990**, *112*, 3223.
(27) Majumdar, D.; Bhattacharyya, S. P.; Maity, D. K. *Int. J. Quantum Chem.* **1992**, *43*, 567.
(28) Chandra, A. K. *J. Mol. Struct. (THEOCHEM)* **1994**, *312*, 297.
(29) Lendvay, G. *J. Phys. Chem.* **1994**, *98*, 6098.
(30) Lendvay, G. *J. Mol. Struct. (THEOCHEM)* **1988**, *167*, 331.
(31) Ponec, R. *Collect. Czech. Chem. Commun.* **1997**, *62*, 1821.
(32) Revision C. Frisch, M. J.; Truchks, G. W.; Head-Gordon, M.; Gill, P. M. W.; Wong, M. W.; Foresman, J. B.; Johnson, B. G.; Schlegel, H. B.; Robb, M. A.; Replogle, E. S.; Gomperts, R.; Andres, J. L.; Roghavachari, K.; Binkley, J. S.; Gonzalez, C.; Martin, R. L.; Gox, D. J.; DeGrees, D. J.; Baker, J.; Stewart, J. J. P.; Pople, J. A. *GAUSSIAN 92*, Gaussian, Inc.: Pittsburgh, PA, 1992.
(33) Frisch, M. J.; Trucks, G. W.; Schlegel, H. B.; Gill, P. M. W.; Johnson, B. G.; Robb, M. A.; Cheeseman, J. R.; Keith, T.; Peterson, G. A.; Montgomery, J. A.; Raghavachari, K.; Al-Laham, M. A.; Zakrzewski, V. G.; Ortiz, J. V.; Foresman, J. B.; Peng, C. Y.; Ayala, P. Y.; Chen, W.; Wong, M. W.; Andres, J. L.; Replogle, E. S.; Gomperts, R.; Martin, R. L.; Fox, D. J.; Binkley, J. S.; Defrees, D. J.; Baker, J.; Stewart, J. J. P.; Head-Gordon, M.; Gonzalez, C.; Pople, J. A. *GAUSSIAN 94*, Revision B.3; Gaussian, Inc.: Pittsburgh, PA, 1995.
(34) Blowers, P.; Ford, L.; Masel, R. I. *J. Phys. Chem. A*, accepted for publication.
(35) Blowers, P.; Masel, R. I. *Surf. Sci.*, accepted for publication.
(36) Masel, R. I.; Lee, W. T. *J. Catal.* **1997**, *165*, 80.
(37) Lee, W. T.; Masel, R. I. *J. Phys. Chem.* **1996**, *100*, 10945.
(38) Lee, W. T.; Masel, R. I. *J. Phys. Chem.* **1995**, *99*, 9363.